has to be exercised when filling capillaries in order to minimize this problem.

3.10.7. Increasing inorganic crystalline phase content series

Table 3.10.2 reports the RQPA results for six inorganic mixtures with increasing amounts of i-A measured with Mo $K\alpha_1$ (transmission) and Cu $K\alpha_1$ (reflection). The Rietveld plots of the mixture with 4 wt% i-A are shown in Fig. 3.10.6. For most of the samples, the AKLD values (see Table 3.10.2) for Mo $K\alpha_1$ radiation are slightly smaller than the corresponding values obtained for Cu $K\alpha_1$ radiation. For this reason, we can conclude that the Mo $K\alpha_1$ analyses are slightly better than those derived using Cu $K\alpha_1$ radiation.

On the other hand, calcite and gypsum presented preferred orientations, with the axes being [104] and [010], respectively. This effect was modelled using the March–Dollase algorithm. Preferred orientation makes the $0l0$ reflections for gypsum have higher intensities in the Cu $K\alpha_1$ patterns, and smaller intensities in the Mo $K\alpha_1$ patterns, than those calculated from the crystal structure (see insets in Fig. 3.10.6). As a consequence, the refined values for flat samples in reflection and transmission geometries were smaller and larger than 1.0, respectively (Cuesta *et al.*, 2015). Although preferred orientation is present in all patterns, the Cu $K\alpha_1$ patterns were recorded in reflection geometry (flat samples), while the Mo $K\alpha_1$ measurements were collected in transmission (also flat samples). This results in opposite diffraction intensity changes and points towards another (possible) fruitful use: joint refinement of these two types of patterns to counterbalance the effects of preferred orientation in RQPA.

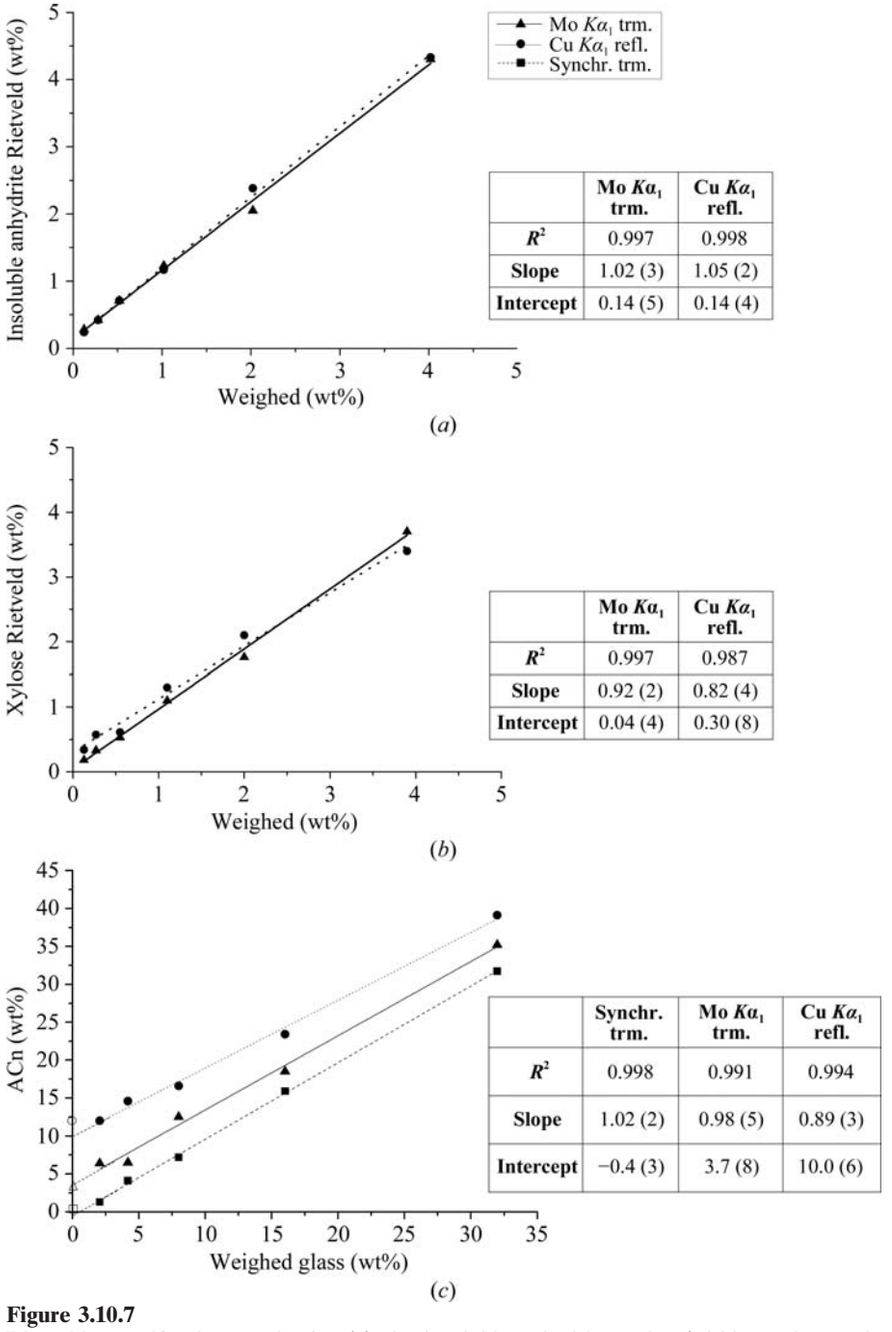

	Mo $K\alpha_1$ trm.	Cu $K\alpha_1$ refl.
R^2	0.997	0.998
Slope	1.02 (3)	1.05 (2)
Intercept	0.14 (5)	0.14 (4)

	Mo $K\alpha_1$ trm.	Cu $K\alpha_1$ refl.
R^2	0.997	0.987
Slope	0.92 (2)	0.82 (4)
Intercept	0.04 (4)	0.30 (8)

	Synchr. trm.	Mo $K\alpha_1$ trm.	Cu $K\alpha_1$ refl.
R^2	0.998	0.991	0.994
Slope	1.02 (2)	0.98 (5)	0.89 (3)
Intercept	−0.4 (3)	3.7 (8)	10.0 (6)

Figure 3.10.7
Rietveld quantification results for (*a*) the insoluble anhydrite series (within an inorganic crystalline matrix), (*b*) the xylose series (within an organic crystalline matrix) and (*c*) the ground-glass series (within an inorganic crystalline matrix) as a function of the weighed amount of each phase. Open symbols represent the derived amorphous contents in the mixtures without any added glass. The results of the least-squares fits are also shown.

Fig. 3.10.7(*a*) shows the quantified i-A contents (wt%), as determined by the Rietveld methodology, as a function of the weighed i-A amount. The two R^2 values for the fits are very close to 1.00, and the intercept values are very close to zero, showing the appropriateness of the Rietveld methodology for quantifying crystalline materials. Furthermore, the slopes of the calibration curves are also 1.00 in both cases. Consequently, this study allows it to be concluded that RQPA for crystalline inorganic phases using powder-diffraction patterns collected using Mo $K\alpha_1$ radiation yields results that are as accurate as those obtained from the well established method using Cu $K\alpha_1$.

3.10.8. Increasing crystalline organic phase content series

Table 3.10.3 shows RQPA results for six mixtures prepared with G, F, L and an increasing amount of X measured with Mo $K\alpha_1$ (transmission) and Cu $K\alpha_1$ (reflection). In general, the values obtained using both radiations are quite similar to the weighed values. The AKLD values and the KLD values for the xylose phase are also reported in Table 3.10.3. The AKLD values from Mo $K\alpha_1$ and Cu $K\alpha_1$ radiations are relatively similar. The main problem for RQPA of organic mixtures measured in reflection geometry is related to the low X-ray absorption of the samples and the transparency effects that lead to poor peak shapes and even some split peaks in the powder patterns, as discussed previously (León-Reina *et al.*, 2016).

Fig. 3.10.7(*b*) shows the quantified xylose contents (wt%) as determined by the Rietveld methodology as a function of the weighed amount of xylose added to the mixtures. The results were plotted to obtain the calibration lines with increasing content of the analyte. Both plots gave R^2 values close to 1.0. However, the slope values were 0.92 and 0.82 for Mo $K\alpha_1$ and Cu $K\alpha_1$ radiations, respec-

Table 3.10.3
RQPA for the crystalline organic mixtures measured with Cu $K\alpha_1$ and Mo $K\alpha_1$ radiations

Weighed amounts (wt%) are also shown for the sake of comparison. Absolute values of the Kullback–Liebler distance (AKLD) for each mixture and the KLD value for xylose are also included. Trm, transmission; rfl, reflection.

	GFL_0.0X			GFL_0.25X			GFL_0.50X		
Phases	wt%	Mo trm	Cu rfl	wt%	Mo trm	Cu rfl	wt%	Mo trm	Cu rfl
G	33.4	33.8 (1)	33.5 (3)	33.3	33.6 (1)	33.1 (2)	33.2	32.3 (2)	33.5 (2)
F	33.5	31.7 (1)	32.7 (3)	33.4	32.3 (1)	34.3 (2)	33.3	32.1 (2)	33.4 (2)
L	33.1	34.5 (1)	33.7 (3)	33.0	33.7 (1)	32.0 (2)	33.0	35.0 (3)	32.5 (2)
X	—	—		0.27	0.33 (4)	0.57 (9)	0.55	0.53 (8)	0.61 (9)
AKLD sum		0.0362	0.0150		0.0216	0.0231		0.0410	0.0096
(X) KLD		—	—		−0.001	−0.002		0.000	−0.001

	GFL_1.0X			GFL_2.0X			GFL_4.0X		
Phases	wt%	Mo trm	Cu rfl	wt%	Mo trm	Cu rfl	wt%	Mo trm	Cu rfl
G	33.0	34.7 (1)	33.6 (2)	32.7	32.2 (1)	31.5 (2)	32.0	32.8 (1)	33.6 (2)
F	33.1	32.6 (1)	33.7 (2)	32.8	31.7 (1)	34.4 (2)	32.2	30.7 (1)	32.5 (2)
L	32.8	31.6 (2)	31.4 (2)	32.5	34.3 (1)	32.0 (2)	31.8	32.9 (1)	30.5 (2)
X	1.1	1.10 (5)	1.3 (1)	2.0	1.76 (5)	2.1 (1)	3.9	3.70 (5)	3.4 (2)
AKLD sum		0.0338	0.0280		0.0363	0.0339		0.0361	0.0372
(X) KLD		0.000	−0.002		0.003	−0.001		0.002	0.005

Table 3.10.4
Rietveld quantitative phase analyses of the CQZ_*x*Gl mixture, where quartz (Q) is the internal standard, to derive amorphous content (am), obtained from SXRPD, Mo $K\alpha_1$ and Cu $K\alpha_1$ patterns

Absolute values of the Kullback–Liebler distance (AKLD) for each mixture and the KLD value for the amorphous content are also included. Trm, transmission; rfl, reflection.

	Weighed			Synchrotron trm				
Mixture	C wt%	Z wt%	Gl wt%	C wt%	Z wt%	Am wt%	AKLD sum	Am KLD
CZQ_0Gl	50.01	49.99	0.00	49.9 (1)	49.6 (1)	0.4 (1)	0.0050	—
CZQ_2Gl	48.98	48.96	2.05	49.7 (1)	49.0 (1)	1.3 (1)	0.0169	0.009
CZQ_4Gl	47.93	47.91	4.17	47.9 (1)	47.6 (1)	4.5 (1)	0.0066	−0.003
CZQ_8Gl	46.00	46.00	7.99	46.6 (1)	45.9 (1)	7.5 (1)	0.0120	0.005
CZQ_16Gl	41.99	41.99	16.01	42.0 (1)	41.6 (1)	16.4 (1)	0.0079	−0.004
CZQ_32Gl	34.00	34.00	31.99	34.0(1)	33.7 (1)	32.3 (1)	0.0061	−0.003

	Mo $K\alpha_1$ trm					Cu $K\alpha_1$ rfl				
Mixture	C wt%	Z wt%	Am wt%	AKLD sum	Am KLD	C wt%	Z wt%	Am wt%	AKLD sum	Am KLD
CZQ_0Gl	47.5 (1)	49.0 (1)	3.5 (1)	0.0358	—	47.2 (1)	40.8 (1)	12.0 (1)	0.1305	—
CZQ_2Gl	45.9 (1)	47.7 (1)	6.4 (1)	0.0679	−0.023	47.4 (1)	40.6 (1)	12.0 (1)	0.1440	−0.036
CZQ_4Gl	46.5 (1)	47.0 (1)	6.5 (1)	0.0422	−0.019	45.8 (1)	39.7 (1)	14.6 (1)	0.1641	−0.052
CZQ_8Gl	42.6 (1)	44.8 (1)	12.5 (1)	0.0832	−0.036	45.3 (1)	38.1 (1)	16.6 (1)	0.1522	−0.058
CZQ_16Gl	39.9 (1)	41.7 (1)	18.5 (1)	0.0475	−0.023	40.9 (1)	35.8 (1)	23.4 (1)	0.1388	−0.061
CZQ_32Gl	31.7 (1)	33.1 (1)	35.2 (1)	0.0635	−0.031	32.2 (1)	28.7 (1)	39.1 (1)	0.1403	−0.064

tively. Slope values close to 1.0 mirror accurate analyses. Furthermore, the *y*-intercept values were 0.04 and 0.30 for Mo $K\alpha_1$ and Cu $K\alpha_1$ radiations, respectively. A *y*-intercept value close to 0.0 mirrors accurate analyses. Hence, it can be concluded that slightly more accurate analyses are obtained for Mo $K\alpha_1$ powder diffraction in transmission when compared with Cu $K\alpha_1$ powder diffraction in reflection for organic crystalline samples.

3.10.9. Increasing amorphous content series within an inorganic crystalline phase matrix

Fig. 3.10.8 shows Mo $K\alpha_1$ (transmission), Cu $K\alpha_1$ (reflection) and SXRPD (transmission) raw patterns for the mixtures with increasing amounts of glass. It is important to highlight that the increase in the background due to the glass is very modest even for ∼32 wt% of glass. Table 3.10.4 shows the RQPA of these mixtures, prepared with C, Z and an increasing amount of Gl, for the three radiations. The glass-free sample may contain amorphous material from the employed phases. Hence, we used the SXRPD data to calculate a correction factor for quartz to yield zero amorphous content for the glass-free sample (León-Reina *et al.*, 2016).

The linear fit to the amorphous content values obtained using SXRPD was very good, R^2 = 0.998, with the slope being 1.00 within the errors (see Fig. 3.10.7*c*). This plot also shows the quantified amorphous contents, in weight percentage, as a function of the amount of added ground glass, measured with Mo $K\alpha_1$ and Cu $K\alpha_1$ radiations. Open symbols indicate the derived amorphous contents obtained with the internal-standard method in the mixture without any added glass, CZQ_0Gl. Both R^2 values are quite close to 1.00, showing the consistency of the internal-standard methodology. However, the slope values were 0.98 and 0.89 for Mo $K\alpha_1$ and Cu $K\alpha_1$ radiations, respectively. Furthermore, the *y*-intercept values were 3.7 and 10.0 for Mo $K\alpha_1$ and Cu $K\alpha_1$ radiations, respectively. Again, slope values close to 1.0 and *y* intercepts close to 0.0 mirror accurate analyses. It must also